ACS APPLIED MATERIALS & INTERFACES

Research Article

www.acsami.org

# Insight into the Interaction of Graphene Oxide with Serum Proteins and the Impact of the Degree of Reduction and Concentration

Xue-Qin Wei,[†] Li-Ying Hao,[†] Xiao-Ru Shao,[†] Quan Zhang,[‡] Xiao-Qin Jia,[†] Zhi-Rong Zhang,[‡] Yun-Feng Lin,*[,†] and Qiang Peng*[,†]

[†]State Key Laboratory of Oral Diseases, West China Hospital of Stomatology, Sichuan University, Chengdu 610041, China

[‡]Key Laboratory of Drug Targeting and Drug Delivery Systems, Ministry of Education, West China School of Pharmacy, Sichuan University, Chengdu 610041, China

Supporting Information

**ABSTRACT:** As novel applied nanomaterials, both graphene oxide (GO) and its reduced form (rGO) have attracted global attention, because of their excellent properties. However, the lack of comprehensive understanding of their interactions with biomacromolecules highly limits their biomedical applications. This work aims to initiate a systematic study on the property changes of GO/rGO upon interaction with serum proteins and on how their degree of reduction and exposure concentration affect this interaction, as well as to analyze the possible biomedical impacts of the interaction. We found that the adsorption of proteins on GO/rGO occurred spontaneously and rapidly, leading to significant changes in size, zeta potential, and morphology. Compared to rGO, GO showed a higher ability in quenching intrinsic fluorescence of serum proteins in a concentration-dependent manner. The protein adsorption efficiency and the types of associated proteins varied, depending on the degree of reduction and concentration of graphene. Our findings indicate the importance of evaluating the potential protein adsorption before making use of GO/rGO in drug delivery, because the changed physicochemical properties after protein adsorption will have significant impacts on safety and effectiveness of these delivery systems. On the other hand, this interaction can also be used for the separation, purification, or delivery of certain proteins.

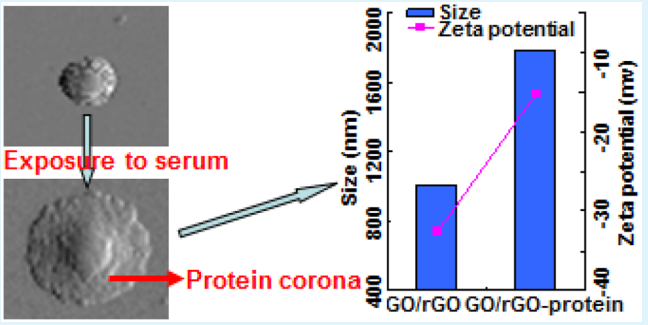


**KEYWORDS:** *graphene oxide, reduced graphene oxide, drug delivery, nanomaterials, protein adsorption, safety*

## INTRODUCTION

The past decades have witnessed the rapid development of various nanomaterials,[1,2] among which graphene oxide (GO) has emerged as an attractive one, because of its outstanding physicochemical properties, such as two-dimension nanostructure, high surface area:volume ratio, strong mechanical properties, and biocompatibility.[3−5] Reports on its applications in drug delivery,[6−10] diagnosis and therapeutics[11−13] have been well-documented, and thus GO has been considered as a potential carrier for practical use in biomedical fields. Although significant progress in developing GO-based drug delivery systems has been made in the past few years, a critical issue is often ignored: the nonspecific interaction of GO with biomacromolecules upon the exposure of GO to biological fluids.

It has been demonstrated that the surface of nanomaterials will be coated with various biomacromolecules immediately after their entry into physiological environment.[14,15] For example, proteins can rapidly adsorb onto nanoparticles and form the so-called "protein coronas".[16−20] The formation of protein coronas will cover the original surface properties of nanomaterials and become the real substance our organs and cells first see.[17,21] As a result, the *in vivo* fate of nanomaterials becomes complicated, no matter how precisely they are initially designed. In addition, the nonspecific interaction may also change the confirmation and function of certain bioactive proteins and thus affect the cell responses and even the immune system.[22−24] Therefore, comprehensive understanding of the interactions between nanomaterials and biological proteins is quite important for better practical use of nanomaterials.

The large surface area:volume ratio and high surface energy of nanomaterials undoubtedly play important roles in facilitating the interaction with proteins. Such interaction will also happen to GO because it also features a large surface area and high surface energy. One recent example is the strong adsorption of lysozyme onto GO via electrostatic attraction and hydrophobic interaction.[25] Undoubtedly, protein adsorption will change the physicochemical properties of GO, such as the size and surface properties, and lead to a loss of its functions.

**Received:** March 2, 2015
**Accepted:** June 1, 2015
**Published:** June 1, 2015





DOI: 10.1021/acsami.5b01874
*ACS Appl. Mater. Interfaces* 2015, 7, 13367−13374

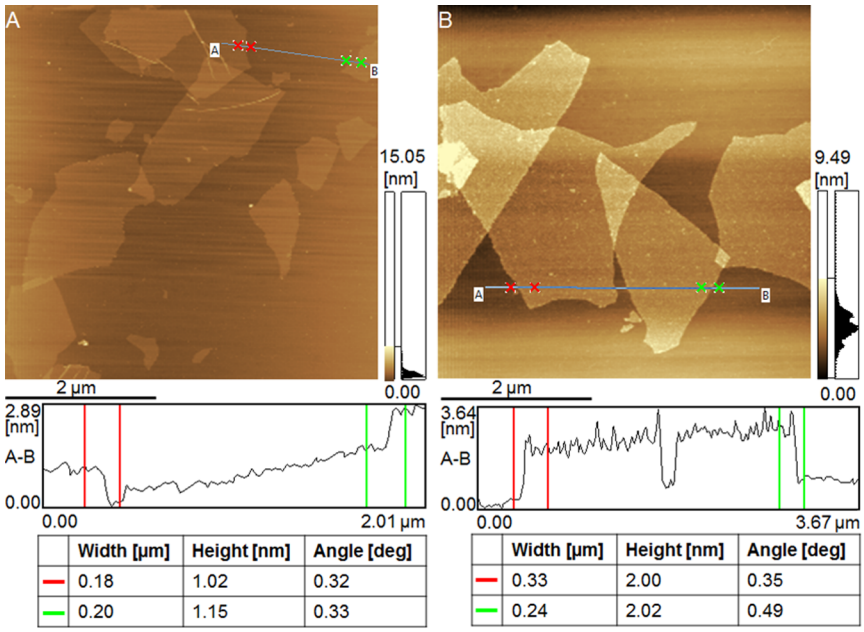


**Figure 1.** Morphology and sheets height of (A) GO and (B) GO−protein complexes characterized by AFM. The height−width profiles show the height change along the specified line. The value of height given in the table indicates the height difference between the two specified points.

More seriously, this interaction may bring risks of capillary blockage resulting from the size increase. Thus, the interaction of GO with serum proteins is a critical factor influencing the safety and effectiveness, and needs thorough consideration before biomedical use. Unfortunately, the lack of systematic studies on GO-serum proteins interaction make us know little about how to use GO in biomedical fields more properly. In addition to GO itself, its reduction form, the reduced GO (rGO), has also been widely used as a carrier for imaging and drug delivery.[26,27] Similarly, a comprehensive understanding of rGO−protein interactions is also required.

Therefore, the main aim of this present work is to investigate the interaction of GO and rGO with serum proteins and the impact of proteins adsorption on their physicochemical properties, and to understand the effects of the degree of GO reduction and exposure concentration on the amount and type of adsorbed proteins. This work provides an insight into the GO/rGO−protein interaction and will be very meaningful for guiding the biomedical use of GO and rGO.

## EXPERIMENTAL SECTION

**Materials.** Graphite powder (Specpure grade) was purchased from Tianjin Guangfu Fine Chemical Research Institute (Tianjin, China). Graphene oxide (GO) was self-made according to Hummer's method.[28] Fetal bovine serum (FBS) was obtained from HyClone (Logan, USA). BCA kit was provided by Beyotime Institute of Biotechnology (Nantong, China). All other chemical reagents used in this study were of analytical grade or better.

**Preparation of Reduced GO (rGO).** The rGO of different degrees of reduction was prepared using an autoclaving method that was developed in our laboratory. Briefly, the GO was suspended in distilled water with concentration of ∼0.2 mg/mL, followed by adjusting the pH value to 11 using NaOH solution. The resultant GO suspension was then placed in an autoclave and sterilized at 121 °C for 20 or 120 min. The obtained rGOs, including rGO (20 min) and rGO (120 min), were adjusted to pH 7.2 using HCl solution for further use.

**Adsorption of FBS Proteins onto GO and rGOs.** The above GO or rGOs suspensions, with concentrations of 10, 20, 40, 80, and 160 μg/mL were ultrasonicated for 30 s before incubating with FBS at room temperature (the FBS concentration was fixed at 2.5% (w/v)). After incubation for 5 min, the resultant GO−protein complexes and rGO−protein complexes were separated by centrifugation at 12 000 rpm for 5 min.

**Atomic Force Microscopy (AFM).** The morphology of GO, rGO, and their complexes with FBS proteins were observed by AFM. All the samples were suspended in distilled water with graphite concentration of 20 μg/mL. One drop of the resulting suspension of each sample was placed on a freshly exfoliated mica sheet. After air drying, the morphology was examined via atomic force microscopy (Model SPM9600, Shimadzu, Japan) using the mode of phase imaging.

**Hydrodynamic Diameter and Zeta Potential.** The hydrodynamic size and zeta potential (ZP) were measured by dynamic light scattering (DLS) and electrophoretic light scattering (ELS) technologies, respectively, on a Zetasizer Nano ZS90 instrument (Malvern Instruments, Ltd., U.K.).[19,29] GO, rGOs, and their complexes with FBS proteins were centrifuged (12 000 rpm, 5 min) and the supernatant was discarded. The pellets washed for three times were resuspended in distilled water for size and zeta potential examination (the graphite concentration of each sample was 160 μg/mL).

**Fluorescence Quenching Effect of GO and rGOs.** After incubation of GO or rGOs with FBS, the resulting suspensions (the final concentration of FBS was fixed at 2.5% and the concentrations of GO or rGOs were 10, 20, 40, 80, and 160 μg/mL) were excited at 270 nm to record the intrinsic fluorescence emission spectrum of FBS proteins within the wavelength range of 290−390 nm (Ex: 270 nm, Em: 290−390 nm).

**Quantification of the Amount of Adsorbed FBS Protein.** The amount of FBS proteins adsorbed on GO or rGOs was determined by BCA assay. Briefly, after incubation for 5 min, the resultant suspension (0.4 mL) was centrifuged at 12 000 rpm for 5 min to separate the formed GO−protein or rGO−protein complexes. An aliquot of 20 μL of supernatant was taken for protein content determination by BCA assay according to the instructions (2.5% FBS served as control). The adsorbed proteins amount was calculated by the following equation:

$$W_{ad} = W_t - W_f$$

where $W_{ad}$ is the amount of adsorbed proteins, $W_t$ is the total amount of proteins, and $W_f$ represents the amount of nonadsorbed proteins in the supernatant. The adsorption efficiency was calculated by another equation:


DOI: 10.1021/acsami.5b01874
ACS Appl. Mater. Interfaces 2015, 7, 13367−13374

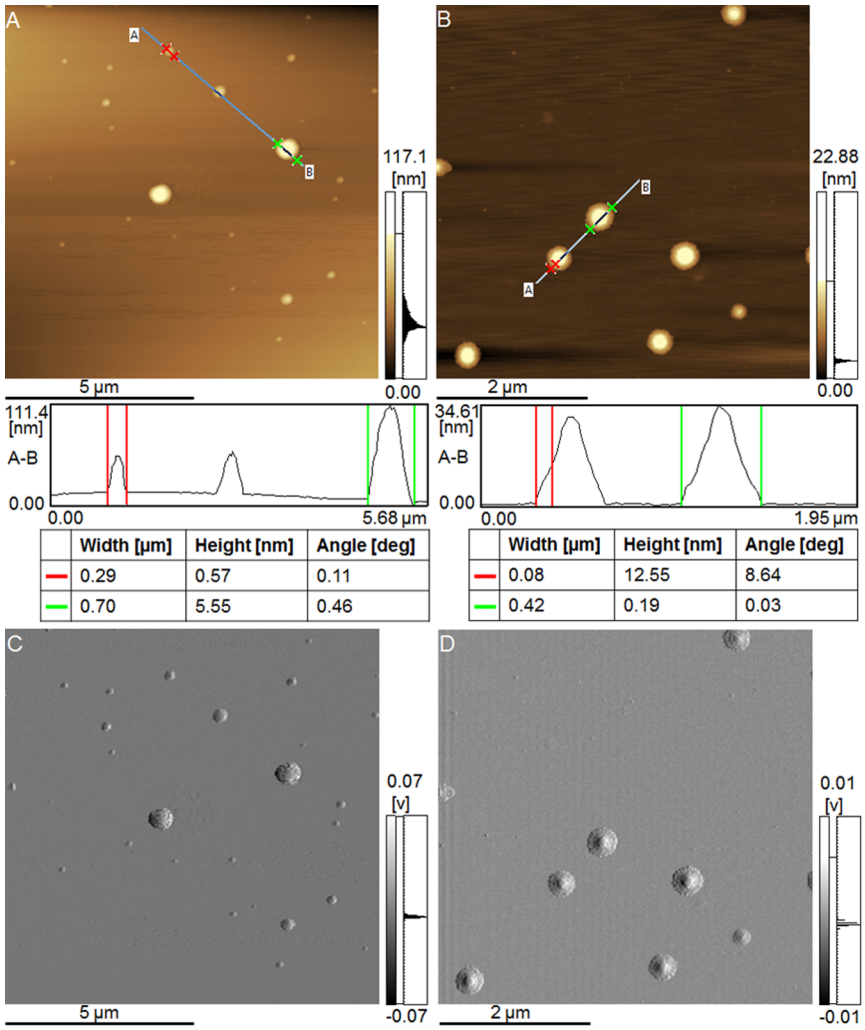


**Figure 2.** AFM images of rGO and rGO−protein complexes obtained by incubating rGO with FBS. (A, B) Height trace image of rGO and rGO−protein complexes, respectively; (C, D), deflection trace image of rGO and rGO−protein complexes, respectively. The height−width profiles in panels A and B present the width of rGO particles and protein coronas.

$$\mathrm{AE} = \frac{W_{\mathrm{ad}}}{W_{\mathrm{g}}}$$

where $W_{\mathrm{ad}}$ is the amount of adsorbed protein, $W_{\mathrm{g}}$ represents the amount of GO or rGO, and AE is the adsorption efficiency.

**Separation of Proteins Adsorbed on GO and rGOs.** The proteins adsorbed on GO and rGOs were separated by 12% SDS-PAGE, according to a previous method.[19] Briefly, GO and rGOs with concentrations of 20 or 160 μg/mL were incubated with FBS as described above. The resultant complexes were collected by centrifugation (12 000 rpm, 5 min), followed by washing with distilled water three times to get rid of the nonadsorbed proteins. The pellets were resuspended in loading buffer and boiled for 3 min. After centrifugation (12 000 rpm, 3 min), the supernatant containing proteins was used for SDS-PAGE and the separated proteins were stained using Coomassie Brilliant Blue.

**Statistical Analysis.** The data in this present work were presented as mean ± s.d. (standard deviation). The statistical difference between groups was examined by one-way analysis of variance, which was considered to be statistically significant when the $P$ value was <0.05.

## RESULTS AND DISCUSSION

In this present work, we prepared two types of rGO with different reduction degrees by adjusting reaction time. The appearance of GO solution changed significantly upon reduction into rGO, because of the enhanced hydrophobicity (see Figure S1-A in the Supporting Information). In addition, the red shift of the absorption peak, which can be observed from GO upon deoxygenation, provides more evidence for the formation of rGO.[30] The UV absorption peak of rGOs showed an obvious red shift compared to GO, and rGO (120 min) had a longer shift than rGO (20 min), indicating the highest degree of reduction of rGO (120 min) followed with rGO (20 min) and GO (Figure S1-B in the Supporting Information). As a result of the reduction, significant differences in physicochemical properties between GO and rGO were observed.

The morphology of GO, rGO, and their complex with FBS proteins were observed via AFM. The GO was monolayer sheets with clean surfaces and a mean sheet height of ∼1 nm (Figure 1A). After incubation with FBS, the obtained GO−protein monolayer had a significant increase in sheet height (∼2 nm) and a decrease in surface cleanliness (Figure 1B), because of the adsorption of proteins onto GO surface. These results indicated that FBS proteins could rapidly adsorb onto GO sheets in a spontaneous manner, leading to the formation of GO−protein complexes.

Unlike the sheet-shape of GO, it was interesting to find rGO was represented by round particles with the width significant


DOI: 10.1021/acsami.5b01874
ACS Appl. Mater. Interfaces 2015, 7, 13367−13374

larger than the height (Figure 2) and having a size range from nanoscale to microscale (see Figure S2 in the Supporting Information). This difference in shape might result from the enhanced hydrophobicity after reduction from GO to rGO. However, there was no difference in shape between rGO (20 min) and rGO (120 min) (Figure S3 in the Supporting Information). The same as GO, rGO also showed significant changes in morphology after incubation with FBS. There was no coating layer surrounding the original rGO particles (Figure 2A). In contrast, a layer of protein coronas surrounding rGO particles could be clearly observed after incubation with FBS (Figure 2B). Particularly, through the height−width profile, the width and height of the formed proteins corona surrounding that specific particle in Figure 2B (red indicators) was ∼80 and 12 nm, respectively. In order to confirm that the outer layer coatings shown in Figure 2B were not hollow, the corresponding Deflection Trace images were recorded. It was quite clear that rGO was solid particles without coating layers (Figure 2C) while protein coronas could be clearly observed for rGO−protein complexes (see Figure 2D and Figure S4 in the Supporting Information). These results suggested that FBS proteins could also adsorb onto rGO spontaneously and rapidly, leading to the formation of protein coronas, as well as the rGO−protein complexes.

In addition to morphology, the size and surface charge of GO and rGO also changed significantly, because of the adsorption of proteins. Figures 2B and 2D provides a visual example of the size change of rGO as the result of protein corona formation. The detailed data of size and zeta potential are shown in Figure 3. The original mean size of GO, rGO (20 min), and rGO (120 min) was 950, 1009, and 1093 nm, respectively, and significantly increased to 1927, 1785, and 1633 nm, respectively, after incubation with FBS (Figure 3A). Meanwhile, the zeta potential of GO, rGO (20 min), and rGO (120 min) was −33, −14, and −15 mV, respectively, and changed to −15, −10, and −13 mV, respectively (Figure 3B) after incubation with FBS. These results could also be considered as evidence for the interaction of GO and rGOs with FBS proteins.

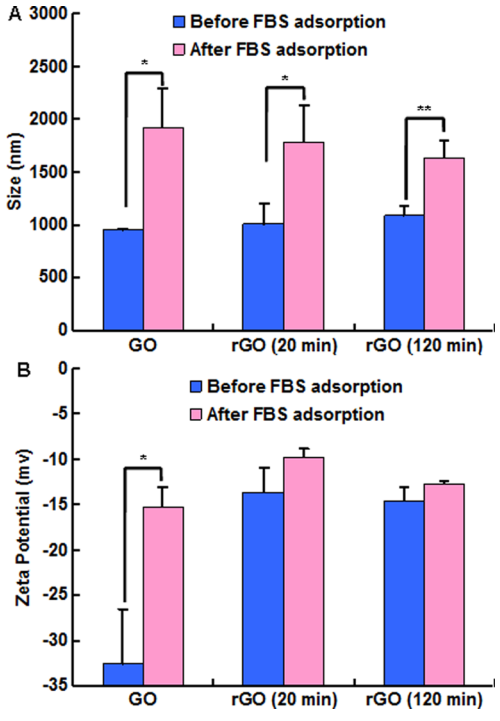


**Figure 3.** Examination of (A) hydrodynamic size and (B) zeta potential of GO/rGOs before or after FBS adsorption. Data are presented as mean ± sd ($n$ = 3). Statistical significance between groups: (*) $p < 0.05$ and (**) $p < 0.01$.

Interestingly, there were significant size changes for both GO and rGOs after FBS adsorption, but only GO presented substantial change in zeta potential (Figure 3). It was speculated according to the morphology (see Figures 1 and 2) that the zeta potentials of both GO−protein and rGO−protein complexes were derived mainly from the adsorbed proteins that were located on the surface of GO/rGOs and presented similar charges. This was considered as the reason for the similar zeta potentials of GO−protein and rGOs−protein complexes, despite the original values. The significant size increase of rGO after incubation with FBS may be largely attributed to the formation of protein coronas surrounding rGO (Figure 2BD). However, protein adsorption may have little direct contribution to the size increase of GO, since the increase in sheet height upon FBS adsorption was only ∼1 nm (Figure 1). However, the zeta potential change that is caused by protein adsorption (from −33 mV to −15 mV, Figure 3B) could strongly weaken the electrostatic repulsive force among GO sheets and thus led to a certain degree of aggregation and resulted in the substantial size increase of GO. This significant size increase must be taken into consideration when GO/rGO is administered intravenously, because too large of a size may enhance the risk of capillary blockage.

On the other hand, the risks or side effects may come from the other side of the coin: the associated proteins. The interaction of proteins with other molecules or surfaces could affect the conformation and properties of associated proteins, like enzymes activity, biological recognition, and interaction with other proteins.[31,32] Our previous work reported the fluorescence quenching of bovine serum albumin upon interaction with a small molecule.[33] Here, we investigated the ability of GO and rGO to quench the fluorescence of FBS proteins. We found that the fluorescent intensity of FBS proteins was strongly reduced upon incubation with as low as 10 μg/mL of GO and further reduced when increasing GO concentrations gradually (Figure 4A). The similar fluorescence quenching of FBS proteins could also be observed when incubating with rGO for 20 min and 120 min (see Figures 4B and 4C). It was noticed that fluorescence quenching was presented in a GO/rGO concentration-dependent manner, indicating that more proteins were involved in the interaction with higher concentrations of GO/rGO. There was also a difference in quenching fluorescence between GO and rGO. The fluorescence quenching efficiency of GO was largely greater than that of rGO with rGO incubated for 120 min being slightly higher than that of rGO incubated for 20 min (Figure 4D). This result implied that GO may have higher affinities to the proteins with intrinsic fluorescence. It was assumed that the different surface properties between GO and rGO, such as hydrophobicity, may confer upon them distinct affinity to different types of proteins.

In order to determine and compare the ability of GO and rGOs in adsorbing FBS proteins, we quantified the amount of adsorbed proteins. As a result, GO and rGOs showed the same trend in adsorbing proteins (Figure 5). The adsorbed proteins amount reached the maximum (∼60 μg) when GO/rGOs were at the highest concentrations (160 μg/mL) and presented a decreasing trend when reducing the GO/rGOs concentrations


DOI: 10.1021/acsami.5b01874
ACS Appl. Mater. Interfaces 2015, 7, 13367−13374

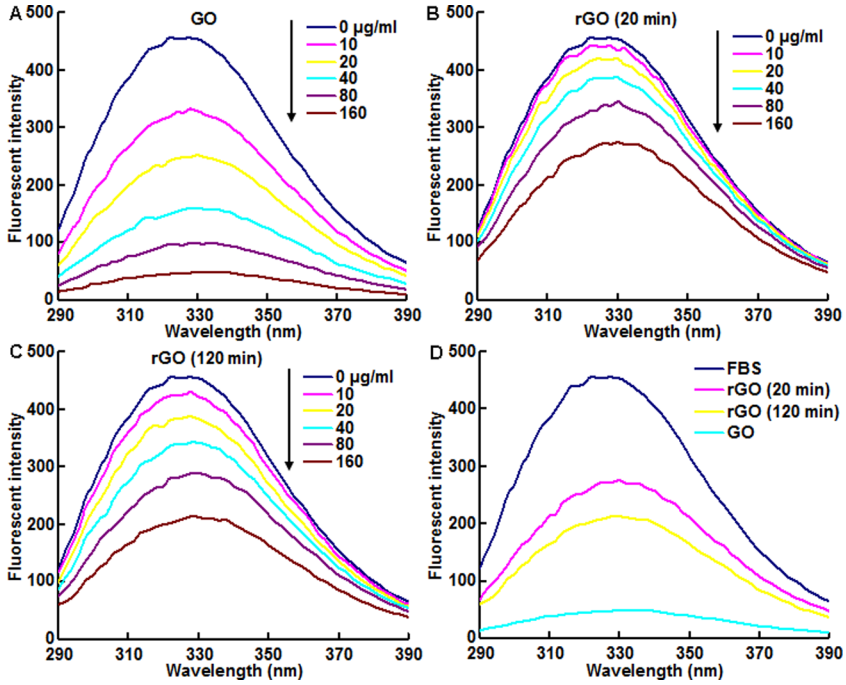


**Figure 4.** Fluorescence quenching of FBS proteins (2.5%, w/v) by incubating with different concentrations of (A) GO, (B) rGO (20 min), and (C) rGO (120 min). (D) Comparison of fluorescence quenching efficiency between GO and rGOs at a GO/rGO concentration of 160 $\mu$g/mL.

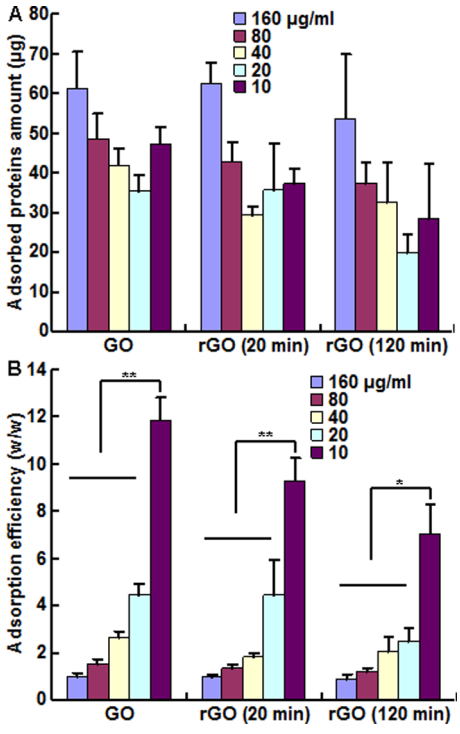


**Figure 5.** (A) Absolute proteins amount adsorbed on GO/rGOs at different concentrations. (B) Protein adsorption efficiency of GO/rGOs. Data are presented as mean ± sd ($n$ = 3). Statistical significance between groups: (*) $p < 0.05$ and (**) $p < 0.01$.

(Figure 5A). However, there was an interesting phenomenon that the amount of proteins adsorbed on both GO and rGOs bounced back at the lowest concentration (10 $\mu$g/mL), suggesting that GO/rGOs may have higher adsorption efficiencies at lower exposure concentrations. Therefore, we figured out their adsorption efficiency at each exposure concentration. The efficiency could be explained as the amount of proteins that every weight unit of GO/rGOs could adsorb. As expected, GO/rGOs showed consistent profiles of adsorption efficiency that was lowest at the highest concentration of GO/rGOs and gradually increased to the maximum with reducing the concentration of GO/rGOs to the minimum 10 $\mu$g/mL (Figure 5B). The above results suggested that (1) GO possessed the highest ability to adsorb serum proteins, followed with rGO (20 min) and then rGO (120 min); (2) an enhanced degree of reduction of GO/rGO could inhibit protein adsorption to some extent; and (3) increasing the exposure concentration of GO/rGO may adsorb more proteins but, in turn, reduce the adsorption efficiency.

It was very interesting to find an opposite order between GO/rGO concentration and protein adsorption efficiency. When a certain amount of proteins (2.5% FBS) were mixed with different concentrations of GO/rGO within a short period of time (5 min), the protein exposure concentration to each sheet or particle would be reduced upon increasing the material concentration. Consequently, a higher protein concentration gradient was present for the GO/rGO with lower concentrations, which facilitated the faster protein adsorption (i.e., the higher adsorption efficiency). In other words, under higher material concentrations, a lesser amount of proteins would be adsorbed on each unit of nanomaterials (for example, each sheet of GO) and more proteins in total within 5 min (Figure 6). This might be the reason for the higher adsorption efficiency at lower material concentration (Figure 5B). The comparison between GO and rGO showed that GO had the higher protein adsorption efficiency, which was probably due to the larger surface area of GO sheets in aqueous solution. Besides, other surface properties, such as charge and hydrophobicity, can also influence protein adsorption efficiency. For instance, GO may adsorb more proteins via $\pi-\pi$ interaction and hydrogen bond, because of its sheet structure and higher hydrophilicity.


DOI: 10.1021/acsami.5b01874
ACS Appl. Mater. Interfaces 2015, 7, 13367−13374

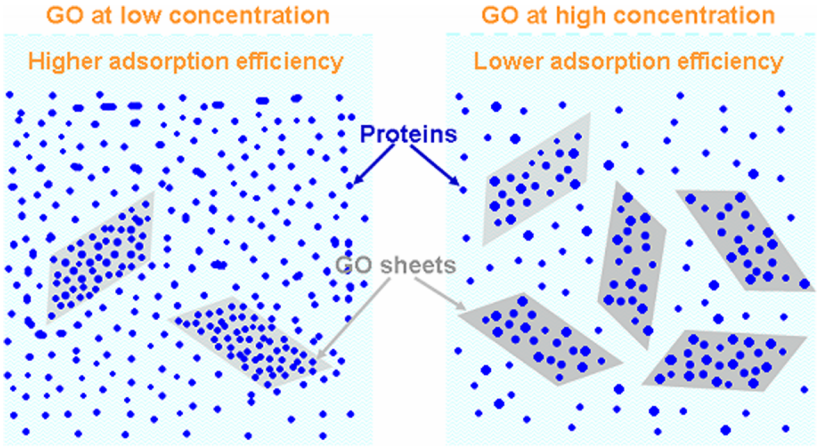


**Figure 6.** Schematic of how the concentration of nanomaterials affects the adsorption of proteins, using GO sheets as an example. At lower GO concentrations, more proteins are adsorbed on each GO sheet (i.e., higher adsorption efficiency) but less proteins in total. At higher GO concentration, however, less proteins are adsorbed on each GO sheet (i.e., lower adsorption efficiency) but more in total.

In addition to the amount of proteins, the type of adsorbed proteins could also be different. Obviously, the mechanisms of protein adsorption on GO/rGO is a type of noncovalent self-assembly, in which some secondary interactions are involved, including van der Waals' force, electrostatic interaction, hydrophobic interaction, $\pi-\pi$ interaction, and hydrogen bonding.[25,34,35] These noncovalent bonds may coexist in the interaction of GO/rGO with proteins, but their contributions may vary, depending on the surface properties of GO/rGO, such as morphology and hydrophobicity. For example, the $\pi-\pi$ interaction may contribute more to the interaction of GO sheets with proteins while hydrophobic interaction may contribute more to rGO−proteins interaction. As a result, this variation in the involved interaction forces would lead to GO/GO adsorbing different types of proteins.

The different proteins adsorbed on GO/rGO were separated via SDS-PAGE. As expected, the type of adsorbed proteins varied significantly, depending on the surface properties and even concentrations of GO/rGO (Figure 7). When the concentration of GO/rGO was 160 $\mu$g/mL, protein bands a, b, and c only appeared in GO−protein complexes (Line 3 in Figure 7) and could not be found in rGO (20 min)−protein complexes (Line 4) or rGO (120 min)−protein complexes (Line 5), indicating these proteins had a relatively strong interaction with GO, perhaps via hydrogen bond and $\pi-\pi$ interaction. In addition, the proteins represented by protein bands b and c have relatively low molecular weight, suggesting that the low-molecular-weight proteins have higher affinity to GO than rGO. Differences also existed between rGOs. As shown in the boxes that are bordered by dotted lines in Figure 7, both rGOs have protein bands d with similar intensity but bands e and f almost only appear in the rGO (20 min)−protein complexes (Line 4), indicating that the proteins represented by protein bands e and f have higher affinity to rGO (20 min), which has lower a degree of reduction than rGO (120 min) and that hydrophobic interaction may not be involved in the interaction of the proteins represented by protein bands e or f with rGO. When the concentration of GO/rGO was 20 $\mu$g/mL, both rGO (20 min)−protein complexes (Line 7) and rGO (120 min)−protein complexes (Line 8) only presented a relatively strong band (h) without the other bands found in the GO−protein complexes (Line 6), indicating that rGOs of 20 $\mu$g/mL had a strong affinity to the protein represented by protein band h and could be used for selectively separation and purification of this protein. Interestingly, material concentration almost had no effect on the type of protein adsorbed on GO (Line 3 vs Line 6) but showed an obvious effect on proteins type adsorbed on rGOs (Lines 4 and 5 vs Lines 7 and 8). The proteins adsorbed on the high concentration of rGOs (Lines 4 and 5) were not adsorbed on the low concentration of rGOs (Lines 7 and 8), implying that different proteins can be extracted using rGOs with varied concentrations.

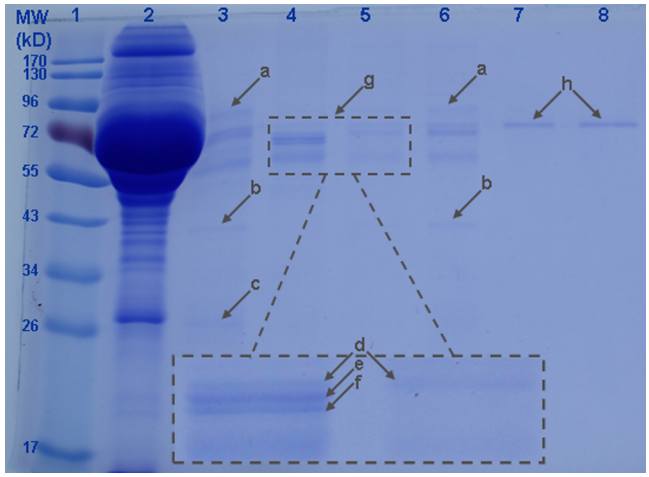


**Figure 7.** 12% SDS-PAGE and Coomassie Brilliant Blue staining of the proteins adsorbed on GO/rGO upon incubation with FBS. [Legend: Line 1, marker; Line 2, diluted FBS; Line 3, GO−protein complexes; Line 4, rGO (20 min)−protein complexes; Line 5, rGO (120 min)−protein complexes (complexes represented by Lines 3−5 were obtained by incubating 160 $\mu$g/mL of GO/rGOs with FBS); Line 6, GO−protein complexes; Line 7, rGO (20 min)−protein complexes; and Line 8, rGO (120 min)−protein complexes (complexes represented by Lines 6−8 were obtained by incubating 20 $\mu$g/mL of GO/rGOs with FBS. Arrows a−h indicate different protein bands; the bands enclosed by box g, bordered by dotted lines, is magnified to highlight bands d, e and f.

SDS-PAGE is an important and convenient qualitative method to identify the type of protein adsorbed on the nanomaterials.[18,25,36,37] The results shown above demonstrated that the type of protein adsorbed varied, according to the degree of reduction and exposure concentration of GO/rGOs.


DOI: 10.1021/acsami.5b01874
ACS Appl. Mater. Interfaces 2015, 7, 13367−13374

It is relatively easy to understand the influence of the degree of reduction on the type of protein adsorbed. As discussed above, the shape and surface properties are different between GO and rGOs. Accordingly, their interactions with proteins are also different, leading to the varied amount and type of the adsorbed proteins. However, the mechanisms underlying the influence of the concentration of rGOs on the type of protein adsorbed are not very clear. It is assumed that a certain type of protein that exists in a small amount in FBS but has a high affinity to rGO may rapidly saturate rGO of low concentration. At high rGO concentrations, however, this type of protein could not saturate rGO, because of the decreased adsorption efficiency and the increased rGO amount, and thus other proteins would become more competitive and could find more space to adsorb onto rGO.

GO/rGO belongs to the promising carriers for delivering drugs. For instance, doxorubicin and paclitaxel have been loaded onto the modified GO for better anticancer effects.[6,7] Nevertheless, the interaction of GO/rGO with proteins should be taken into consideration for better understanding and control of their *in vivo* performance, as well as for safe delivery. Our findings suggested that the adsorption of proteins on GO/rGO occurred rapidly and would lead to significant changes in their physicochemical properties. These results are meaningful for guiding the practical use of GO/rGO-based systems in biomedical fields. First, increasing material concentration can enhance the total amount of adsorbed proteins but will reduce the adsorption efficiency, which means lower concentration would be better when GO/rGO systems aim at concentrating proteins. Second, it is necessary to select an appropriate material concentration to reduce the amount of adsorbed proteins to the largest extent. Third, much attention needs to be paid when GO- or rGO-based systems are designed for intravenous injection since the significant size increase upon interaction with serum proteins would bring high risks of capillary blockage.

## CONCLUSION

Much attention has been paid to the interaction of nanomaterials with proteins, because of its significant effects on the physicochemical and biological properties of both nanomaterials and associated proteins. Our results show that the nanomaterials−-proteins interaction can cause changes in the size, zeta potential, and morphology of GO and rGOs. Meanwhile, it can also lead to fluorescence quenching of FBS proteins. There are several noncovalent forces involved in the interaction, which is dependent on the degree of reduction and concentration of GO and rGOs. Accordingly, the amount and type of adsorbed proteins are varied. This work provides an insight into the interaction of serum proteins with GO/rGO and evaluates the impacts of the degree of reduction and exposure concentration. Our findings disclose the possible biomedical impacts of GO/rGO. First, a lower concentration of GO/rGO is beneficial to concentrating proteins, because of its higher adsorption efficiency at lower concentration. Particularly, GO/rGO has different selectivity to proteins, which can be used for the separation and purification of certain proteins. Second, selecting an appropriate concentration of GO/rGO is important to minimize the amount of adsorbed proteins when GO/rGO serves as a carrier for the delivery of other drugs. Most importantly, protein adsorption must be taken into consideration when GO- or rGO-based systems are designed for intravenous injection since the significant size increase upon interaction with serum proteins would bring high risks of capillary blockage. On the other hand, this strong interaction of GO/rGO with proteins can be utilized for long-term delivery of certain protein therapeutics.

## ASSOCIATED CONTENT

### Supporting Information

Characterizations of GO/rGO by UV and AFM. The Supporting Information is available free of charge on the ACS Publications website at DOI: 10.1021/acsami.5b01874.

## AUTHOR INFORMATION

### Corresponding Authors

*Tel.: +86 28 85503487. Fax: +86 28 85503487. E-mail: yunfenglin@scu.edu.cn (Y.-F. Lin).

*Tel.: +86 28 85501484. Fax: +86 28 85501484. E-mail: lijm2002@163.com (Q. Peng).

### Notes

The authors declare no competing financial interest.

## ACKNOWLEDGMENTS

This work was supported by National Natural Science Foundation of China (Nos. 81402860, 81470721, 31170929) and Sichuan Science and Technology Innovation Team (No. 2014TD0001).

## REFERENCES

(1) Kamaly, N.; Xiao, Z.; Valencia, P. M.; Radovic-Moreno, A. F.; Farokhzad, O. C. Targeted Polymeric Therapeutic Nanoparticles: Design, Development and Clinical Translation. *Chem. Soc. Rev.* **2012**, *41* (7), 2971−3010.

(2) Scheinberg, D. A.; Villa, C. H.; Escorcia, F. E.; McDevitt, M. R. Conscripts of the Infinite Armada: Systemic Cancer Therapy Using Nanomaterials. *Nat. Rev. Clin. Oncol.* **2010**, *7* (5), 266−276.

(3) Zhu, Y.; Murali, S.; Cai, W.; Li, X.; Suk, J. W.; Potts, J. R.; Ruoff, R. S. Graphene and Graphene Oxide: Synthesis, Properties, and Applications. *Adv. Mater.* **2010**, *22* (35), 3906−3924.

(4) Chung, C.; Kim, Y. K.; Shin, D.; Ryoo, S. R.; Hong, B. H.; Min, D. H. Biomedical Applications of Graphene and Graphene Oxide. *Acc. Chem. Res.* **2013**, *46* (10), 2211−2224.

(5) Krishna, K. V.; Menard-Moyon, C.; Verma, S.; Bianco, A. Graphene-Based Nanomaterials for Nanobiotechnology and Biomedical Applications. *Nanomedicine (London, U.K.)* **2013**, *8* (10), 1669−1688.

(6) Zhou, T.; Zhou, X.; Xing, D. Controlled Release of Doxorubicin from Graphene Oxide Based Charge-Reversal Nanocarrier. *Biomaterials* **2014**, *35* (13), 4185−4194.

(7) Xu, Z.; Wang, S.; Li, Y.; Wang, M.; Shi, P.; Huang, X. Covalent Functionalization of Graphene Oxide with Biocompatible Poly(ethylene Glycol) for Delivery of Paclitaxel. *ACS Appl. Mater. Interfaces* **2014**, *6* (19), 17268−17276.

(8) Song, E.; Han, W.; Li, C.; Cheng, D.; Li, L.; Liu, L.; Zhu, G.; Song, Y.; Tan, W. Hyaluronic Acid-Decorated Graphene Oxide Nanohybrids as Nanocarriers for Targeted and Ph-Responsive Anticancer Drug Delivery. *ACS Appl. Mater. Interfaces* **2014**, *6* (15), 11882−11890.

(9) Kurapati, R.; Raichur, A. M. Near-Infrared Light-Responsive Graphene Oxide Composite Multilayer Capsules: A Novel Route for Remote Controlled Drug Delivery. *Chem. Commun. (Cambridge, U.K.)* **2013**, *49* (7), 734−736.

(10) Liu, J.; Cui, L.; Losic, D. Graphene and Graphene Oxide as New Nanocarriers for Drug Delivery Applications. *Acta Biomater.* **2013**, *9* (12), 9243−9257.

(11) Cho, Y.; Choi, Y. Graphene Oxide-Photosensitizer Conjugate as a Redox-Responsive Theranostic Agent. *Chem. Commun. (Cambridge, U.K.)* **2012**, *48* (79), 9912−9914.



DOI: 10.1021/acsami.5b01874
*ACS Appl. Mater. Interfaces* 2015, 7, 13367−13374

(12) Yang, K.; Feng, L.; Shi, X.; Liu, Z. Nano-Graphene in Biomedicine: Theranostic Applications. *Chem. Soc. Rev.* **2013**, *42* (2), 530−547.
(13) Feng, L.; Wu, L.; Qu, X. New Horizons for Diagnostics and Therapeutic Applications of Graphene and Graphene Oxide. *Adv. Mater.* **2013**, *25* (2), 168−186.
(14) Walkey, C. D.; Chan, W. C. Understanding and Controlling the Interaction of Nanomaterials with Proteins in a Physiological Environment. *Chem. Soc. Rev.* **2012**, *41* (7), 2780−2799.
(15) Monopoli, M. P.; Aberg, C.; Salvati, A.; Dawson, K. A. Biomolecular Coronas Provide the Biological Identity of Nanosized Materials. *Nat. Nanotechnol.* **2012**, *7* (12), 779−786.
(16) Lindman, S.; Lynch, I.; Thulin, E.; Nilsson, H.; Dawson, K. A.; Linse, S. Systematic Investigation of the Thermodynamics of Hsa Adsorption to *N*-Iso-Propylacrylamide/*N*-*tert*-Butylacrylamide Copolymer Nanoparticles. Effects of Particle Size and Hydrophobicity. *Nano Lett.* **2007**, *7* (4), 914−920.
(17) Walczyk, D.; Bombelli, F. B.; Monopoli, M. P.; Lynch, I.; Dawson, K. A. What the Cell "Sees" in Bionanoscience. *J. Am. Chem. Soc.* **2010**, *132* (16), 5761−5768.
(18) Lundqvist, M.; Stigler, J.; Elia, G.; Lynch, I.; Cedervall, T.; Dawson, K. A. Nanoparticle Size and Surface Properties Determine the Protein Corona with Possible Implications for Biological Impacts. *Proc. Natl. Acad. Sci. U. S. A.* **2008**, *105* (38), 14265−14270.
(19) Peng, Q.; Zhang, S.; Yang, Q.; Zhang, T.; Wei, X. Q.; Jiang, L.; Zhang, C. L.; Chen, Q. M.; Zhang, Z. R.; Lin, Y. F. Preformed Albumin Corona, a Protective Coating for Nanoparticles Based Drug Delivery System. *Biomaterials* **2013**, *34* (33), 8521−8530.
(20) Borgognoni, C. F.; Mormann, M.; Qu, Y.; Schafer, M.; Langer, K.; Ozturk, C.; Wagner, S.; Chen, C.; Zhao, Y.; Fuchs, H.; Riehemann, K. Reaction of Human Macrophages on Protein Corona Covered $TiO_2$ Nanoparticles. *Nanomedicine* **2015**, *11* (2), 275−282.
(21) Ge, C.; Du, J.; Zhao, L.; Wang, L.; Liu, Y.; Li, D.; Yang, Y.; Zhou, R.; Zhao, Y.; Chai, Z.; Chen, C. Binding of Blood Proteins to Carbon Nanotubes Reduces Cytotoxicity. *Proc. Natl. Acad. Sci. U.S.A.* **2011**, *108* (41), 16968−16973.
(22) Zolnik, B. S.; Gonzalez-Fernandez, A.; Sadrieh, N.; Dobrovolskaia, M. A. Nanoparticles and the Immune System. *Endocrinology* **2010**, *151* (2), 458−465.
(23) Li, N.; Xia, T.; Nel, A. E. The Role of Oxidative Stress in Ambient Particulate Matter-Induced Lung Diseases and Its Implications in the Toxicity of Engineered Nanoparticles. *Free Radical Biol. Med.* **2008**, *44* (9), 1689−1699.
(24) Deng, Z. J.; Liang, M.; Monteiro, M.; Toth, I.; Minchin, R. F. Nanoparticle-Induced Unfolding of Fibrinogen Promotes Mac-1 Receptor Activation and Inflammation. *Nat. Nanotechnol.* **2011**, *6* (1), 39−44.
(25) Li, S.; Mulloor, J. J.; Wang, L.; Ji, Y.; Mulloor, C. J.; Micic, M.; Orbulescu, J.; Leblanc, R. M. Strong and Selective Adsorption of Lysozyme on Graphene Oxide. *ACS Appl. Mater. Interfaces* **2014**, *6* (8), 5704−5712.
(26) Shi, S.; Yang, K.; Hong, H.; Valdovinos, H. F.; Nayak, T. R.; Zhang, Y.; Theuer, C. P.; Barnhart, T. E.; Liu, Z.; Cai, W. Tumor Vasculature Targeting and Imaging in Living Mice with Reduced Graphene Oxide. *Biomaterials* **2013**, *34* (12), 3002−3009.
(27) Wang, Y.; Polavarapu, L.; Liz-Marzán, L. M. Reduced Graphene Oxide-Supported Gold Nanostars for Improved SERS Sensing and Drug Delivery. *ACS Appl. Mater. Interfaces* **2014**, *6* (24), 21798−21805.
(28) Hummers, W. S.; Offeman, R. E. Preparation of Graphitic Oxide. *J. Am. Chem. Soc.* **1958**, *80* (6), 1339−1339.
(29) Peng, Q.; Wei, X. Q.; Shao, X. R.; Zhang, T.; Zhang, S.; Fu, N.; Cai, X. X.; Zhang, Z. R.; Lin, Y. F. Nanocomplex Based on Biocompatible Phospholipids and Albumin for Long-Circulation Applications. *ACS Appl. Mater. Interfaces* **2014**, *6* (16), 13730−13737.
(30) Gurunathan, S.; Han, J. W.; Kim, J. H. Green Chemistry Approach for the Synthesis of Biocompatible Graphene. *Int. J. Nanomed.* **2013**, *8*, 2719−2732.
(31) Shemetov, A. A.; Nabiev, I.; Sukhanova, A. Molecular Interaction of Proteins and Peptides with Nanoparticles. *ACS Nano* **2012**, *6* (6), 4585−4602.
(32) Shao, Q.; Qian, Y.; Wu, P.; Zhang, H.; Cai, C. Graphene Oxide-Induced Conformation Changes of Glucose Oxidase Studied by Infrared Spectroscopy. *Colloids Surf., B* **2013**, *109*, 115−120.
(33) Peng, Q.; Wei, X. Q.; Yang, Q.; Zhang, S.; Zhang, T.; Shao, X. R.; Cai, X. X.; Zhang, Z. R.; Lin, Y. F. Enhanced Biostability of Nanoparticle-Based Drug Delivery Systems by Albumin Corona. *Nanomedicine (London, U.K.)* **2015**, *10* (2), 205−214.
(34) Zhang, Y.; Zhang, J.; Huang, X.; Zhou, X.; Wu, H.; Guo, S. Assembly of Graphene Oxide−Enzyme Conjugates through Hydrophobic Interaction. *Small* **2012**, *8* (1), 154−159.
(35) Zhou, L.; Jiang, Y.; Gao, J.; Zhao, X.; Ma, L. Graphene Oxide as a Matrix for the Immobilization of Glucose Oxidase. *Appl. Biochem. Biotechnol.* **2012**, *168* (6), 1635−1642.
(36) Lundqvist, M.; Stigler, J.; Cedervall, T.; Berggard, T.; Flanagan, M. B.; Lynch, I.; Elia, G.; Dawson, K. The Evolution of the Protein Corona around Nanoparticles: A Test Study. *ACS Nano* **2011**, *5* (9), 7503−7509.
(37) Cedervall, T.; Lynch, I.; Lindman, S.; Berggard, T.; Thulin, E.; Nilsson, H.; Dawson, K. A.; Linse, S. Understanding the Nanoparticle-Protein Corona Using Methods to Quantify Exchange Rates and Affinities of Proteins for Nanoparticles. *Proc. Natl. Acad. Sci. U.S.A.* **2007**, *104* (7), 2050−2055.


DOI: 10.1021/acsami.5b01874
*ACS Appl. Mater. Interfaces* 2015, 7, 13367−13374